

# Preparation and in vitro evaluation of doxorubicin-loaded $\text{Fe}_3\text{O}_4$ magnetic nanoparticles modified with biocompatible copolymers

Abolfazl Akbarzadeh<sup>1</sup>Haleh Mikaeili<sup>2</sup>Nosratollah Zarghami<sup>3</sup>Rahmati Mohammad<sup>3</sup>Amin Barkhordari<sup>3</sup>Soodabeh Davaran<sup>2</sup><sup>1</sup>Drug Applied Research Center,<sup>2</sup>Tuberculosis and Lung Disease Research Center of Tabriz,<sup>3</sup>Department of Clinical Biochemistry and Laboratory Medicine, Division of Medical Biotechnology, Faculty of Medicine, Tabriz University of Medical Sciences, Tabriz, Iran

**Background:** Superparamagnetic iron oxide nanoparticles are attractive materials that have been widely used in medicine for drug delivery, diagnostic imaging, and therapeutic applications. In our study, superparamagnetic iron oxide nanoparticles and the anticancer drug, doxorubicin hydrochloride, were encapsulated into poly (D, L-lactide-co-glycolic acid) poly (ethylene glycol) (PLGA-PEG) nanoparticles for local treatment. The magnetic properties conferred by superparamagnetic iron oxide nanoparticles could help to maintain the nanoparticles in the joint with an external magnetic field.

**Methods:** A series of PLGA:PEG triblock copolymers were synthesized by ring-opening polymerization of D, L-lactide and glycolide with different molecular weights of polyethylene glycol (PEG<sub>2000</sub>, PEG<sub>3000</sub>, and PEG<sub>4000</sub>) as an initiator. The bulk properties of these copolymers were characterized using <sup>1</sup>H nuclear magnetic resonance spectroscopy, gel permeation chromatography, Fourier transform infrared spectroscopy, and differential scanning calorimetry. In addition, the resulting particles were characterized by x-ray powder diffraction, scanning electron microscopy, and vibrating sample magnetometry.

**Results:** The doxorubicin encapsulation amount was reduced for PLGA:PEG<sub>2000</sub> and PLGA:PEG<sub>3000</sub> triblock copolymers, but increased to a great extent for PLGA:PEG<sub>4000</sub> triblock copolymer. This is due to the increased water uptake capacity of the blended triblock copolymer, which encapsulated more doxorubicin molecules into a swollen copolymer matrix. The drug encapsulation efficiency achieved for  $\text{Fe}_3\text{O}_4$  magnetic nanoparticles modified with PLGA:PEG<sub>2000</sub>, PLGA:PEG<sub>3000</sub>, and PLGA:PEG<sub>4000</sub> copolymers was 69.5%, 73%, and 78%, respectively, and the release kinetics were controlled. The in vitro cytotoxicity test showed that the  $\text{Fe}_3\text{O}_4$ -PLGA:PEG<sub>4000</sub> magnetic nanoparticles had no cytotoxicity and were biocompatible.

**Conclusion:** There is potential for use of these nanoparticles for biomedical application. Future work includes in vivo investigation of the targeting capability and effectiveness of these nanoparticles in the treatment of lung cancer.

**Keywords:** superparamagnetic iron oxide nanoparticles, triblock copolymer, doxorubicin encapsulation, water uptake, drug encapsulation efficiency

## Introduction

Magnetic nanoparticles are a major class of nanoscale materials with the potential to revolutionize current clinical diagnostic and therapeutic techniques. Due to their unique physical properties and ability to function at the cellular and molecular level of biological interactions, magnetic nanoparticles are being actively investigated as the next generation of magnetic resonance imaging contrast agents<sup>1</sup> and as carriers for targeted drug delivery.<sup>2,3</sup> Although early research in the field can be dated back several decades, a recent surge of interest in nanotechnology has significantly expanded the

Correspondence: Soodabeh Davaran  
Tuberculosis and Lung Disease Research  
Center of Tabriz, Tabriz University  
of Medical Sciences, Tabriz, Iran  
Tel +98 41 1337 2250  
Fax +98 41 1334 4798  
Email davaran@tbzmed.ac.ir

breadth and depth of magnetic nanoparticle research. With a wide range of applications in the detection, diagnosis, treatment of illnesses such as cancer,<sup>4</sup> cardiovascular disease,<sup>5</sup> and neurological disease,<sup>6</sup> magnetic nanoparticles may soon play a significant role in meeting tomorrow's health care needs.

As therapeutic tools, magnetic nanoparticles have been evaluated extensively for targeted delivery of pharmaceuticals through magnetic drug targeting<sup>7,8</sup> and by active targeting through the attachment of high affinity ligands.<sup>9–11</sup> With the ability to utilize magnetic attraction or specific targeting of disease biomarkers, magnetic nanoparticles offer an attractive means of remotely directing therapeutic agents specifically to a disease site, while simultaneously reducing dosage and the deleterious side effects associated with nonspecific uptake of cytotoxic drugs by healthy tissue. Also referred to as magnetic targeted carriers, colloidal iron oxide particles in early clinical trials have demonstrated some degree of success with the technique and shown satisfactory toleration by patients.<sup>12,13</sup> Although not yet capable of reaching levels of safety and efficacy for regulatory approval, preclinical studies indicate that some of the shortcomings of magnetic drug targeting technology, such as poor penetration depth and diffusion of the released drug from the disease site, can be overcome by improvements in magnetic targeted carrier design.<sup>14</sup> Furthermore, use of magnetic nanoparticles as carriers in multifunctional nanoplateforms as a means of real-time monitoring of drug delivery is an area of intense interest.<sup>15</sup>

A significant challenge associated with the application of these magnetic nanoparticle systems is their behavior in vivo. The efficacy of many such systems is often compromised due to recognition and clearance by the reticuloendothelial system prior to reaching the target tissue, as well as by an inability to overcome biological barriers, such as the vascular endothelium or the blood-brain barrier. The fate of these magnetic nanoparticles upon intravenous administration is highly dependent on their size, morphology, charge, and surface chemistry. These physicochemical properties of nanoparticles greatly affect their subsequent pharmacokinetics and biodistribution.<sup>18</sup> To increase the effectiveness of magnetic nanoparticles, several techniques, including reducing size and grafting nonfouling polymers, have been employed to improve their “stealthiness” and increase their blood circulation time to maximize the likelihood of reaching targeted tissues.<sup>19,20</sup>

The major disadvantage of most chemotherapeutic approaches to cancer treatment is that most of them are nonspecific. Therapeutic (generally cytotoxic) drugs are administered intravenously, leading to general systemic

distribution (Figure 1). The nonspecific nature of this technique results in the well known side effects of chemotherapy because the cytotoxic drug attacks normal healthy cells in addition to its primary target and tumor cells.<sup>21,22</sup> Magnetic nanoparticles can be used to overcome this great disadvantage. Nanoparticles can be used to treat tumors in three different ways: specific antibodies can be conjugated to the magnetic nanoparticles to bind selectively to related receptors and inhibit tumor growth; targeted magnetic nanoparticles can be used via hyperthermia for tumor therapy; and drugs can be loaded onto the magnetic nanoparticles for targeted therapy.<sup>23–25</sup> The targeted delivery of antitumor agents adsorbed on the surface of magnetic nanoparticles is a promising alternative to conventional chemotherapy. The particles loaded with the drug are concentrated at the target site with the aid of an external magnet. The drugs are then released at the desired area. Magnetic particles smaller than 4  $\mu\text{m}$  are eliminated by cells of the reticuloendothelial system, mainly in the liver (60%–90%) and spleen (3%–10%). Particles larger than 200 nm are usually filtered to the spleen, the cutoff point of which extends up to 250 nm. Particles up to 100 nm are mainly phagocytosed via liver cells. In general, the larger the particles, the shorter their plasma half-life.<sup>27</sup>

Functionalization of magnetic nanoparticles with amino groups, silica, polymers, various surfactants, or other organic compounds is usually done in order to achieve better physicochemical properties. Moreover, the core/shell structures of magnetic nanoparticles have the advantages

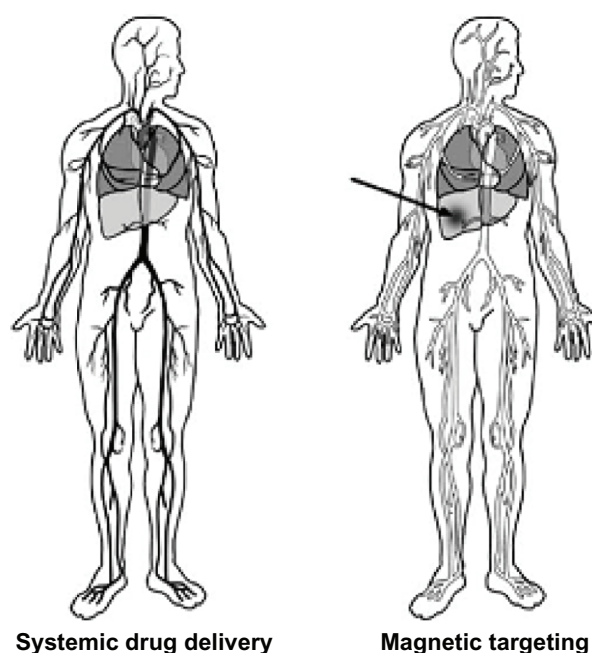


Figure 1 Concept of magnetic drug targeting.<sup>20</sup>

of good dispersion, high stability against oxidation, and an appreciable amount of drug can be loaded into the polymer shell. Furthermore, lots of functional groups from polymers on the surface can be used for further functionalization to obtain various properties.<sup>28</sup> It is preferable that magnetic nanoparticles retain sufficient hydrophilicity with coating, and do not exceed 100 nm in size in order to avoid rapid clearance by the reticuloendothelial system.<sup>29</sup> It was found that surface functionalization also plays a key role in nanoparticle toxicity.<sup>30</sup>

Poly (L-lactic acid) (PLLA) and its copolymers with glycolic acid, poly (D,L-lactic-co-glycolic acid) (PLGA) have been extensively used as biodegradable carriers for drug delivery<sup>31,32</sup> and as temporal scaffolds for tissue engineering.<sup>33,34</sup> These biodegradable aliphatic polyesters with proven biocompatibility have versatile biodegradation properties depending on their molecular weight and chemical compositions.<sup>35</sup> Nevertheless, there have been many attempts to improve the properties of the copolymer to make them suitable for a specific application. For example, to prolong the circulation time of PLGA nanoparticles in the blood stream in vivo, PLLA:poly(ethylene glycol) (PEG) triblock copolymers were coated onto the surface of PLGA nanoparticles by simple blending of PLLA-PEG triblock copolymer with PLGA during the nanoparticle formulation process.<sup>36</sup>

The aim of the present work was to assess the merits of  $\text{Fe}_3\text{O}_4$ -PLGA-PEG nanoparticles as anticancer drug carrier. For this purpose, magnetic  $\text{Fe}_3\text{O}_4$  nanoparticles were first prepared and then the copolymer PLGA-PEG was synthesized with PEG of various molecular weights (Figure 2).

Copolymer was confirmed with  $^1\text{H}$  nuclear magnetic resonance (NMR), differential scanning calorimetry (DSC), and Fourier transform infrared (FTIR) spectra. Molecular weight was determined by gel permeation chromatography. Doxorubicin was chosen for the encapsulation studies in nanoparticles made of  $\text{Fe}_3\text{O}_4$ -PLGA-PEG due to its well known physical/chemical properties and low cost.<sup>37,38</sup> Doxorubicin was encapsulated within nanoparticles made of  $\text{Fe}_3\text{O}_4$ -PLGA-PEG using the double emulsion method (w/o/w). The nanoparticles were characterized in terms of size, in vitro cytotoxicity, and in vitro release of doxorubicin.<sup>39</sup>

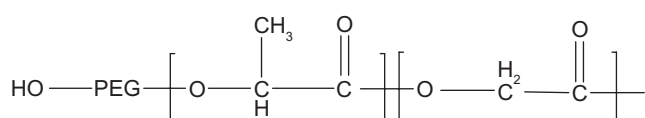


**Figure 2** Structure of the PEG-PLGA copolymer.

**Abbreviations:** PEG, poly (ethylene glycol); PLGA, poly (D, L-lactic-co-glycolic acid).

## Materials and methods

### Materials

Ferric chloride hexahydrate ( $\text{FeCl}_3 \cdot 6\text{H}_2\text{O}$ ), ferrous chloride tetrahydrate ( $\text{FeCl}_2 \cdot 4\text{H}_2\text{O}$ ), and ammonium hydroxide (25 wt%) were purchased from Fluka (Buchs, Switzerland). D, L-lactide and glycolide were purchased from Sigma-Aldrich (St Louis, MO) and recrystallized with ethyl acetate. Stannous octoate ( $\text{Sn}(\text{Oct})_2$ ; stannous 2-ethylhexanoate), PEG (molecular weight 2000, 3000, and 4000), and dimethyl sulfoxide were purchased from Sigma-Aldrich. PEGs were dehydrated under vacuum at  $70^\circ\text{C}$  for 12 hours and used without further purification. Doxorubicin hydrochloride was purchased from Sigma-Aldrich. X-ray diffraction (Rigaku D/MAX-2400 x-ray diffractometer with Ni-filtered  $\text{Cu K}\alpha$  radiation), and scanning electron microscopy (SEM) measurements were conducted using VEGA/TESEM XL DS2 measurements were conducted using the Perkin Elmer series. The drug-loading capacity and release behavior were determined using an ultraviolet-visible 2550 spectrometer (Shimadzu, Tokyo, Japan). Infrared spectra were recorded in real-time with a Perkin Elmer series FTIR. The magnetic property was measured on a vibrating sample magnetometer (Meghnatis Daghigh Kavir, Iran) at room temperature.  $^1\text{H}$  NMR spectra was recorded in real-time with a Bruker DRX 300 spectrometer operating at  $300.13\text{ MHz}$ . The average molecular weight was obtained by gel permeation chromatography performed in dichloromethane ( $\text{CH}_2\text{Cl}_2$ ) with a Waters Associates Model ALC/gel permeation chromatography 244 apparatus. The samples were homogenated using a homogenizer (SilentCrusher M, Heidolph Instruments GmbH, Schwabach, Germany). The organic phase was evaporated by rotary (Rotary Evaporators, Heidolph Instruments, Hei-VAP series).

### Synthesis of superparamagnetic magnetic nanoparticles

Superparamagnetic magnetic nanoparticles were prepared using an improved chemical coprecipitation method.<sup>40</sup> According to this method, 3.1736 g of  $\text{FeCl}_2 \cdot 4\text{H}_2\text{O}$  (0.016 mol) and 7.5684 g of  $\text{FeCl}_3 \cdot 6\text{H}_2\text{O}$  (0.028 mol) were dissolved in 320 mL of deionized water, such that  $\text{Fe}^{2+}/\text{Fe}^{3+} = 1/1.75$ . The mixed solution was stirred under nitrogen at  $80^\circ\text{C}$  for 1 hour (Figure 3A). Then,  $\text{NH}_3 \cdot \text{H}_2\text{O}$  40 mL was injected into the mixture rapidly, stirred under nitrogen for another hour, and then cooled to room temperature (Figure 3B). The precipitated particles were washed five times with hot water and separated by magnetic decantation (Figure 3C). Finally, the magnetic nanoparticles were dried under vacuum at  $70^\circ\text{C}$ .

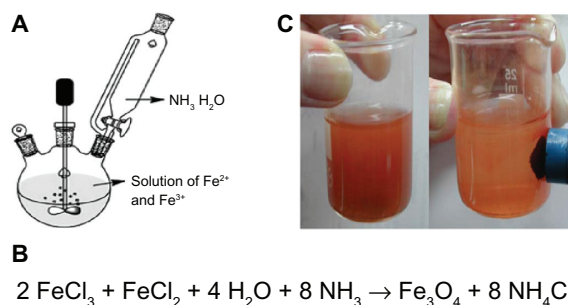


**Figure 3** (A) Reactor of synthesis of superparamagnetic magnetite nanoparticles, (B) preparation of  $\text{Fe}_3\text{O}_4$  magnetite nanoparticles, and (C) magnetite-hexane suspension attached to a magnet.

### Preparation of PLGA-PEG triblock copolymer

PLGA-PEG copolymers with different molecular weights of PEG (PEG<sub>2000</sub>, PEG<sub>3000</sub>, and PEG<sub>4000</sub>) as an initiator were prepared by a melt polymerization process under vacuum using stannous octoate [ $\text{Sn}(\text{Oct})_2$ ; stannous 2-ethylhexanoate] as a catalyst.<sup>41</sup> DL-lactide (14.4 g), glycolide (3.86 g), and PEG<sub>2000</sub> or PEG<sub>3000</sub> or PEG<sub>4000</sub> 8 g (45% w/w) in a bottleneck

flask were heated to 140°C under a nitrogen atmosphere for complete melting. The molar ratio of DL-lactide and glycolide was 3:1. Then 0.05% (w/w) stannous octoate was added and the temperature of the reaction mixture was raised to 180°C. The temperature was maintained for 4 hours. The polymerization was carried out under vacuum. The copolymer was recovered by dissolution in methylene chloride followed by precipitation in ice-cold diethyl ether. The synthesis process of PLGA-PEG copolymer is shown in Figure 4A. A triblock copolymer of PLGA-PEG was prepared by ring opening polymerization of DL-lactide and glycolide in the presence of PEG<sub>2000</sub>, PEG<sub>3000</sub>, and PEG<sub>4000</sub> (Figure 4B).<sup>42</sup>

### Measurement of copolymer

The  $^1\text{H}$  NMR spectra were recorded in  $\text{CDCl}_3$  on a Bruker AM 300.13 MHz spectrometer. The FTIR (Perkin Elmer series) spectrum was obtained from a neat film cast of the chloroform copolymer solution between KBr tablets. Gel permeation chromatography was performed in dichloromethane

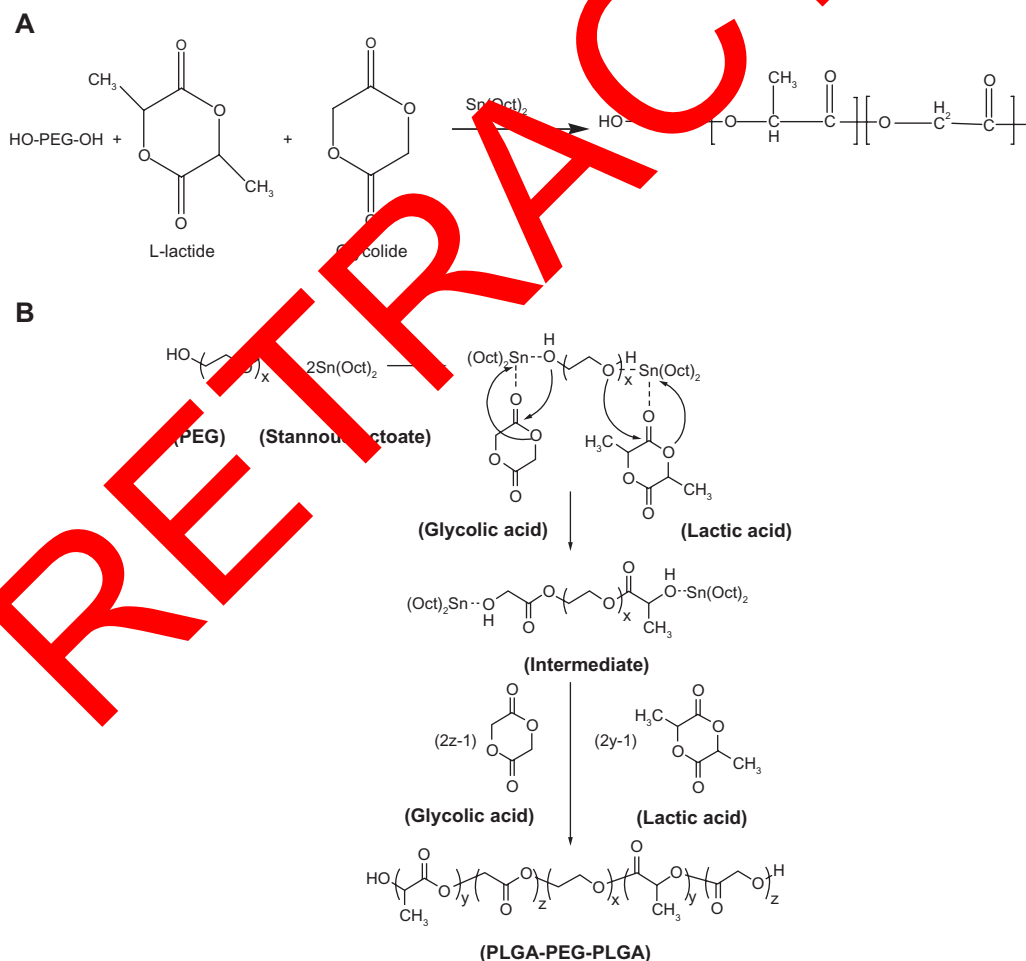


**Figure 4** (A) Preparation of a triblock copolymer of PLGA-PEG, and (B) mechanism of PLGA-PEG prepared by  $\text{Sn}(\text{Oct})_2$  as catalyst.<sup>42</sup>  
**Abbreviations:** PEG, poly (ethylene glycol); PLGA, poly (D, L-lactic-co-glycolic acid).

using a Waters Associates (Milford, MA) Model ALC/gel permeation chromatography 244 apparatus. The molecular weight and molecular weight distribution of the copolymer were calculated using polystyrene as the standard. The thermogram characteristics of selected batches of nanoparticles were determined by DSC thermogram analysis (Perkin Elmer 7 series) on the glass transition temperature or melting point.

### Doxorubicin-loaded $\text{Fe}_3\text{O}_4$ magnetic nanoparticles modified with PLGA-PEG copolymers

Doxorubicin-loaded  $\text{Fe}_3\text{O}_4$  magnetic nanoparticles modified with PLGA-PEG copolymers were prepared using the double emulsion method (w/o/w) employed by Song et al<sup>43</sup> with minor modifications. An aqueous solution of doxorubicin 5 mg/5 mL was emulsified in 10 mL dichloromethane, in which 120 mg of the copolymer and 4 mg magnetic nanoparticles had been dissolved, using a probe homogenizer or sonication at 20,000 rpm for 30 seconds. This w/o emulsion was transferred to a 50 mL aqueous solution of polyvinyl alcohol 1% and the mixture was probe-homogenized (or sonicated) at 72,000 rpm for one minute. The w/o/w emulsion formed was gently stirred at room temperature until evaporation of the organic phase was completed or the organic phase was evaporated (Heidolph Instruments). The nanoparticles were purified by applying two cycles of centrifugation (12,000 rpm for 1 hour in a Biofuge 28 RS, Heraeus Centrifuge) and reconstituted with deionized and distilled water. The nanoparticles were finally filtered through 0.2  $\mu\text{m}$  filter (Millipore, Bedford, MA). In order to increase doxorubicin entrapment in the nanoparticles, the external aqueous phase used during the

second emulsification step was saturated with doxorubicin. Blank nanoparticles were also prepared by the same method without adding doxorubicin at any stage of the preparation (Figure 5).<sup>44</sup>

### Drug loading and determination of doxorubicin entrapment efficiency

Doxorubicin, an anticancer drug, was used for the drug loading and release studies. In brief, 20 mg of lyophilized nanoparticles and 5 mg of doxorubicin were dispersed in phosphate-buffered solution. The solution was stirred at 4°C for 3 days to allow doxorubicin to entrap within the nanoparticle network. This value was then compared with the total amount of doxorubicin to determine the doxorubicin loading efficiency of the nanoparticles. The amount of nonentrapped doxorubicin in aqueous phase was determined using an ultraviolet (255 nm  $\lambda_{\text{ex}}$ , 470 nm and  $\lambda_{\text{em}}$  585 nm) spectrophotometer (Shimadzu). This procedure permits analysis of a doxorubicin solution with removal of most interfering substances.<sup>45</sup> The amount of doxorubicin entrapped within the nanoparticles was calculated by the difference between the total amount used to prepare the nanoparticles and the amount of doxorubicin present in the aqueous phase, using the following formula:

$$\text{Loading efficiency \%} = \left[ \frac{\text{(amount of loaded drug in mg)}}{\text{(amount of added drug in mg)}} \right] \times 100\%$$

### In vitro drug release kinetics study

To study the drug release profile of the synthesized doxorubicin-loaded  $\text{Fe}_3\text{O}_4$  magnetic nanoparticles modified with

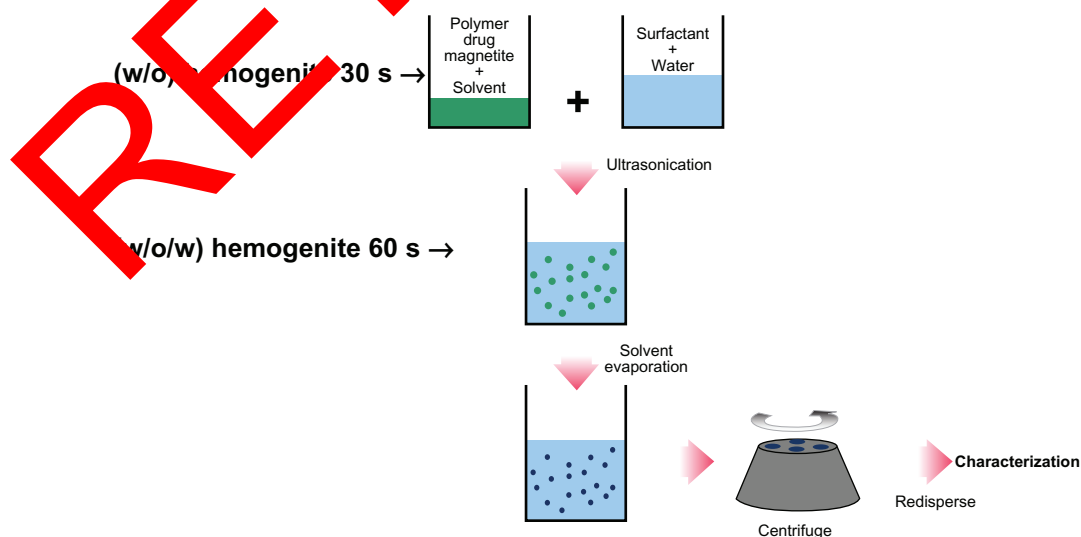


**Figure 5** Process of w/o/w double emulsion method.<sup>44</sup>



PLGA-PEG copolymers, 3 mg of drug-loaded nanoparticles were dispersed in 30 mL of phosphate-buffered solution (pH 7.4) and acetate buffer (pH 8, the pH value for survey pH-dependent and pH sensitivity of drug release kinetics). Samples were incubated at various temperatures from 37°C to 40°C. At designated time intervals, a 3 mL sample was removed and same volume was reconstituted by adding 3 mL of fresh phosphate-buffered solution and acetate buffer to each sample. After the experiment, the samples were analyzed using ultraviolet spectrofluorometry to determine the amount of doxorubicin released ( $\lambda_{\text{ex}}$  470 nm and  $\lambda_{\text{em}}$  585 nm for doxorubicin measurement).<sup>46</sup>

## Cell culture

### In vitro cytotoxicity and cell culture study

An A549 lung cancer cell line (kindly donated by the Pharmaceutical Nanotechnology Research Center, Tabriz University of Medical Sciences, Tabriz, Iran) was cultured in RPMI1640 (Gibco, Invitrogen, Carlsbad, CA) supplemented with 10% heat-inactivated fetal bovine serum (Gibco, Invitrogen), 2 mg/mL sodium bicarbonate, 0.05 mg/mL penicillin G (Serva, Germany), 0.08 mg/mL streptomycin (Merck, Germany) and incubated at 37°C with humidified air containing 5% CO<sub>2</sub>. After culturing a sufficient amount of cells, the cytotoxic effect of Fe<sub>3</sub>O<sub>4</sub>-PLGA-PEG<sub>4000</sub> was studied using 24-hour, 48-hour, and 72-hour MTT assays.<sup>47</sup> Briefly, 1000 cells/well were cultivated in 96-well plate. After 24 hours of incubation at 37°C in a humidified atmosphere containing 5% CO<sub>2</sub>, the cells were treated with serial concentrations of Fe<sub>3</sub>O<sub>4</sub>-PLGA-PEG<sub>4000</sub>-doxorubicin (0 mg/mL to 0.57 mg/mL) for 24, 48, and 72 hours in a quadruplicate manner, while cells treated with 0 mg/mL extract and 200  $\mu$ L culture medium containing 10% dimethylsulfoxide served as a control (Figure 6). After incubation, the medium

in all wells of the plate was replaced with fresh medium and the cells were left for 24 hours in an incubator. The medium in all the wells was then removed carefully, and 50  $\mu$ L of 2 mg/mL MTT (Sigma-Aldrich) dissolved in phosphate-buffered solution was added to each well, and the plate was covered with aluminum foil and incubated for 4.5 hours. After removing the contents of the wells, 200  $\mu$ L of pure dimethylsulfoxide was added to the wells. Sorensen's glycine buffer 25  $\mu$ L was then added and the absorbance of each well was immediately read at 570 nm using an EL  $\times$  800 microplate absorbance reader (Bio-Tek Instruments, Winooski, VT) with a reference wavelength of 630 nm.<sup>48</sup>

### Cell treatment

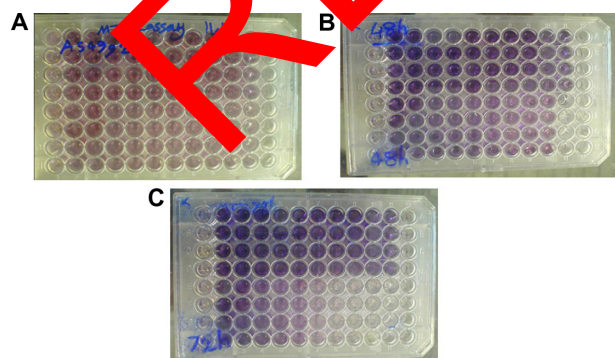
After determination of IC<sub>50</sub>,  $1 \times 10^6$  cells were treated with serial concentrations of Fe<sub>3</sub>O<sub>4</sub>-PLGA-PEG<sub>4000</sub>-doxorubicin (0.028, 0.057, 0.114, 0.142, 0.171, and 0.199 mg/mL). For the control cells, the same volume of 10% dimethylsulfoxide without Fe<sub>3</sub>O<sub>4</sub>-PLGA-PEG<sub>4000</sub>-doxorubicin was added to the flask containing control cells. The culture flasks were then incubated at 37°C containing 5% CO<sub>2</sub> using a humidified atmosphere incubator for a 24-hour exposure duration (Figure 7).

### Nanoparticle characterization

Power x-ray diffraction (Rigaku D/MAX-2400 x-ray diffractometer with Ni-filtered Cu K $\alpha$  radiation) was used to investigate the crystal structure of the magnetic nanoparticles. The size and shape of the nanoparticles was determined by SEM. The sample was dispersed in ethanol and a small drop was spread onto a 400 mesh copper grid. The thermogram characteristics of selected batches of nanoparticles were determined by DSC thermogram analysis (Perkin Elmer 7 series) on the glass transition temperature or melting point. The magnetization curves of the samples were measured using vibrating sample magnetometry at room temperature. The infrared spectra were recorded by a FTIR spectrophotometer (Perkin Elmer series), and the sample and KBr were pressed to form a tablet. <sup>1</sup>H NMR spectra were recorded in real-time with a Bruker DRX 300 spectrometer operating at 300.13 MHz.

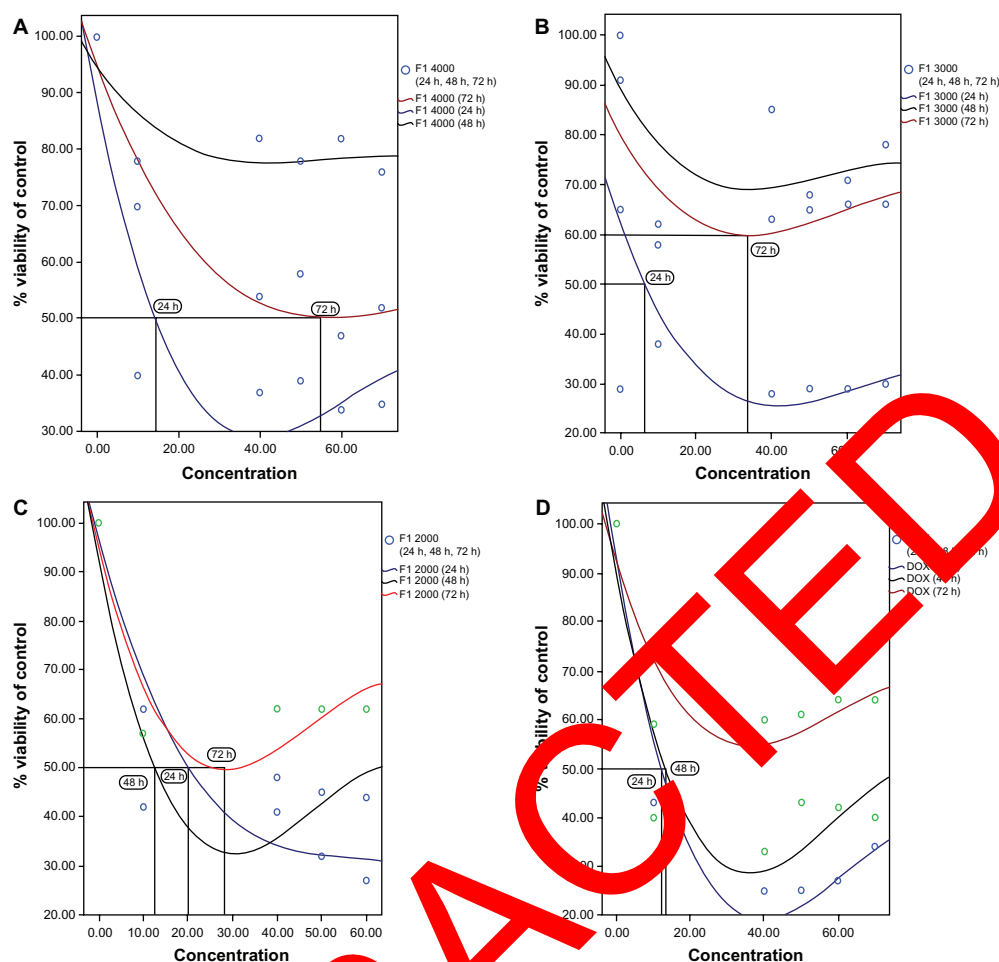
### X-ray diffraction patterns

Figure 8 shows the x-ray diffraction patterns for pure Fe<sub>3</sub>O<sub>4</sub> and doxorubicin-loaded Fe<sub>3</sub>O<sub>4</sub> magnetic nanoparticles modified with PLGA-PEG copolymers. It is apparent that the diffraction pattern for our Fe<sub>3</sub>O<sub>4</sub> nanoparticles is close to the standard pattern for crystalline magnetite. The characteristic



**Figure 6** Cytotoxic effect of Fe<sub>3</sub>O<sub>4</sub>-PLGA-PEG<sub>4000</sub> on A549 lung cancer cell line after 24 hours (A), 48 hours (B), and 72 hours (C) exposure.

**Abbreviations:** PEG, poly (ethylene glycol); PLGA, poly (D, L-lactic-co-glycolic acid).



**Figure 7**  $\text{IC}_{50}$  of (A)  $\text{Fe}_3\text{O}_4$ -PLGA-PEG<sub>4000</sub>-doxorubicin, (B)  $\text{Fe}_3\text{O}_4$ -PLGA-PEG<sub>3000</sub>-doxorubicin, (C)  $\text{Fe}_3\text{O}_4$ -PLGA-PEG<sub>2000</sub>-doxorubicin, and (D) pure doxorubicin on A549 tumor cell line after 24, 48, and 72 hours of treatment.

**Abbreviations:** PEG, poly (ethylene glycol); PLGA, poly (D, L-lactide-co-glycolide).

diffraction peaks are marked, respectively, by their indices (220), (311), (400), (422), (511), and (640), which could be well indexed to the inverse cubic spinel structure of  $\text{Fe}_3\text{O}_4$  (JCPDS card 85-1336). Characteristic diffraction peaks were also observed for doxorubicin-loaded  $\text{Fe}_3\text{O}_4$  magnetic nanoparticles modified with PLGA-PEG copolymers. This demonstrates that modification of the  $\text{Fe}_3\text{O}_4$  nanoparticles did not lead to a crystal phase change. The average crystallite size  $D$  was about 15 nm and obtained from the Sherrer equation  $D = K\lambda/(\beta \cos \theta)$ , where  $K$  is the constant,  $\lambda$  is the x-ray wavelength, and  $\beta$  is the peak width of half-maximum.<sup>49</sup>

### Size and size distribution

The surface morphology of the nanospheres during the incubation period was observed by SEM. The nanographs of pure  $\text{Fe}_3\text{O}_4$  nanoparticles (Figure 9A), PLGA-PEG copolymers (Figure 9B), and doxorubicin-loaded  $\text{Fe}_3\text{O}_4$  magnetic nanoparticles modified with PLGA-PEG copolymers

(Figure 9C) are shown. Observing the photograph, it can be seen that the nanoparticles were well aggregated, which was due to the nanosize of the  $\text{Fe}_3\text{O}_4$  of about 20 nm. After encapsulation and modification of the doxorubicin-loaded  $\text{Fe}_3\text{O}_4$  magnetic nanoparticles with PLGA-PEG copolymers, the size of the particles changed to 25–75 nm and dispersion of the particles was greatly improved (Figure 9B and C), which can be explained by the electrostatic repulsion force and steric hindrance between the copolymer chains on the encapsulated  $\text{Fe}_3\text{O}_4$  nanoparticles. The samples were coated with gold particles.<sup>50</sup>

### DSC analysis

The thermogram characteristics of selected batches of nanoparticles determined by DSC thermogram analysis (Perkin Elmer 7 series) of glass transition temperature or melting point is shown (Figure 10). All the samples were placed in an aluminum pan and scanned from 35°C to 250°C with a heat-

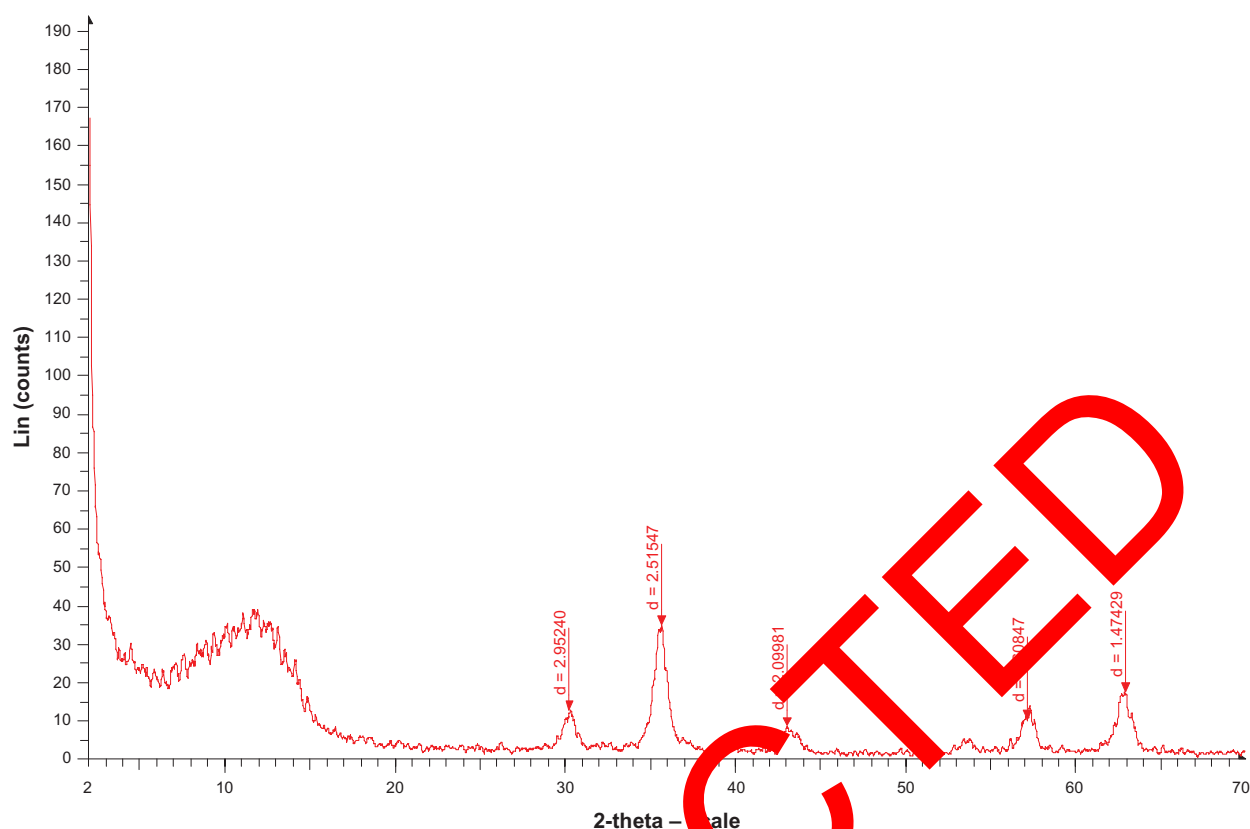


**Figure 8** X-ray diffraction patterns of pure  $\text{Fe}_3\text{O}_4$  nanoparticles.

ing rate of  $20^\circ\text{C}$  per minute. All the DSC thermograms were cooled back to  $200^\circ\text{C}$  at the same rate. After 5 minutes obtained from the first heating cycle. Nitrogen was used as a sweeping gas. Samples (8 mg) were equilibrated at  $250^\circ\text{C}$  and purged with pure dry nitrogen at a flow rate of  $40\text{ mL/minute}$ . The nitrogen was heated to  $120^\circ\text{C}$  at  $10^\circ\text{C}$  per minute, after which it was held isothermally for 3 minutes. The samples were cooled back to  $200^\circ\text{C}$  at the same rate. After 5 minutes at the isothermal stage, the second heating cycle proceeded at a  $5^\circ\text{C}$  per minute temperature ramp speed to  $120^\circ\text{C}$ . The glass transition temperature of the polymer was obtained by taking the midpoint of the slope during glass transition. In the present research, two heating cycles were conducted.

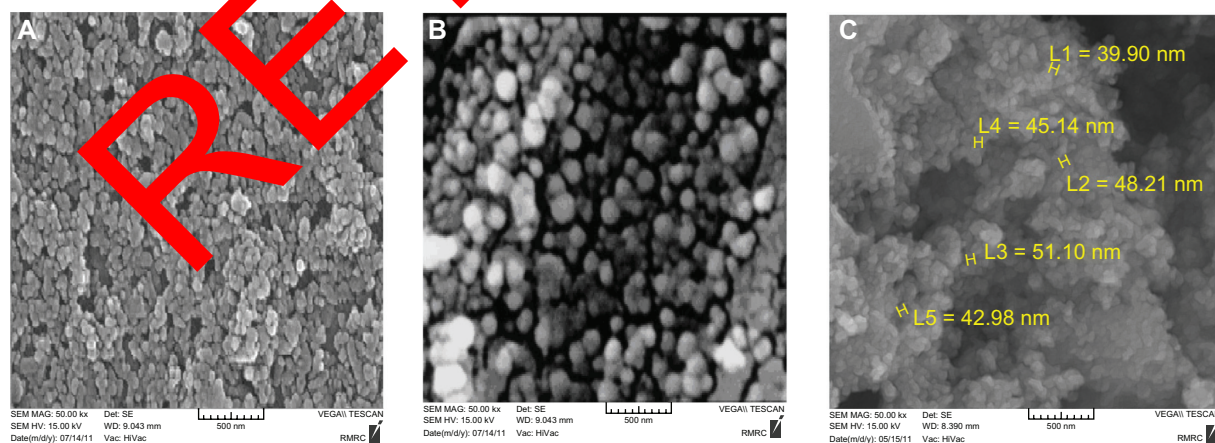


**Figure 9** Scanning electron microscopy of (A)  $\text{Fe}_3\text{O}_4$  magnetic nanoparticles, (B) PLGA-PEG nanoparticles, and (C) doxorubicin-loaded  $\text{Fe}_3\text{O}_4$  magnetic nanoparticles modified with PLGA-PEG copolymers.

**Abbreviations:** PEG, poly (ethylene glycol); PLGA, poly (D, L-lactic-co-glycolic acid).



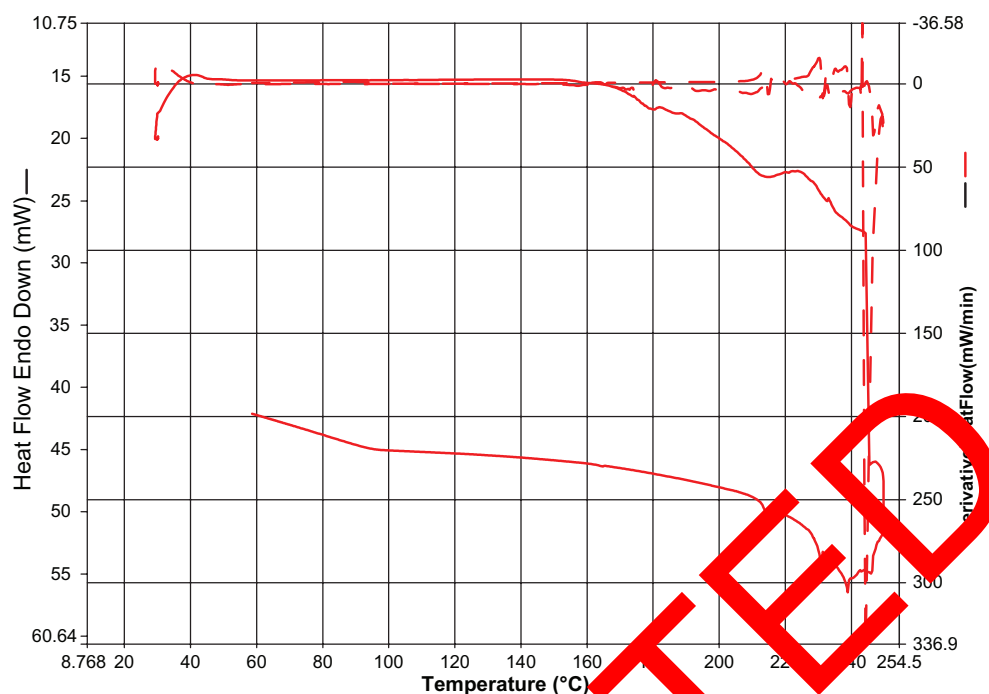


**Figure 10** Thermogram characteristics of selected batches of nanoparticles.

Indium was used as the standard reference material to calibrate the temperature and energy scales of the DSC instrument. As a control, the pure material was analyzed to observe changes in melting point or glass transition temperature.<sup>51</sup>

### Magnetism test

The magnetic properties of the nanoparticles were analyzed by vibrating sample magnetometry at room temperature.<sup>52</sup> Figure 11 shows the hysteresis loops of the samples. The saturation magnetization was found to be 17.5 emu/g for

doxorubicin-loaded  $\text{Fe}_3\text{O}_4$  magnetic nanoparticles modified with PLGA-PEG copolymers, ie, less than for the pure  $\text{Fe}_3\text{O}_4$  nanoparticles (70.9 emu/g). This difference suggests that a large amount of polymer encapsulated the  $\text{Fe}_3\text{O}_4$  nanoparticles and doxorubicin. With the large saturation magnetization, the doxorubicin-loaded  $\text{Fe}_3\text{O}_4$  magnetic nanoparticles modified with PLGA-PEG copolymers could be separated from the reaction medium rapidly and easily in a magnetic field. In addition, there was no hysteresis in the magnetization, with both remanence and coercivity being zero, suggesting that these magnetic nanoparticles are superparamagnetic. When the external magnetic field was removed, the magnetic nanoparticles could be well dispersed by gentle shaking. These magnetic properties are critical for application in the biomedical and bioengineering fields.

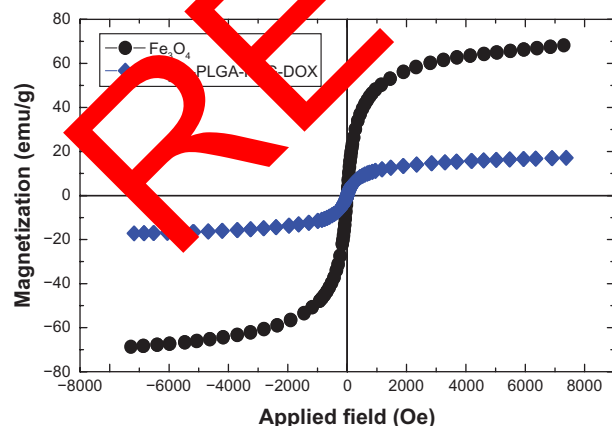


**Figure 11** Magnetic behavior of magnetic nanoparticles.

**Abbreviations:** PLGA-PEG-DOX, Doxorubicin-loaded poly(lactide-co-glycolide)-polyethylene glycol.

## Results

### Measurement and characterization of nanoparticles

#### FTIR spectroscopy

The F-IR spectrum is consistent with the structure of the expected copolymer. FTIR spectroscopy was used to show the structure of  $\text{Fe}_3\text{O}_4$  and PLGA-PEG copolymer nanoparticles. From the infrared spectra shown in Figure 12A, the absorption peaks at  $580\text{ cm}^{-1}$  belonged to the stretching vibration mode of Fe—O bonds in  $\text{Fe}_3\text{O}_4$  (Table 1). Figure 12B

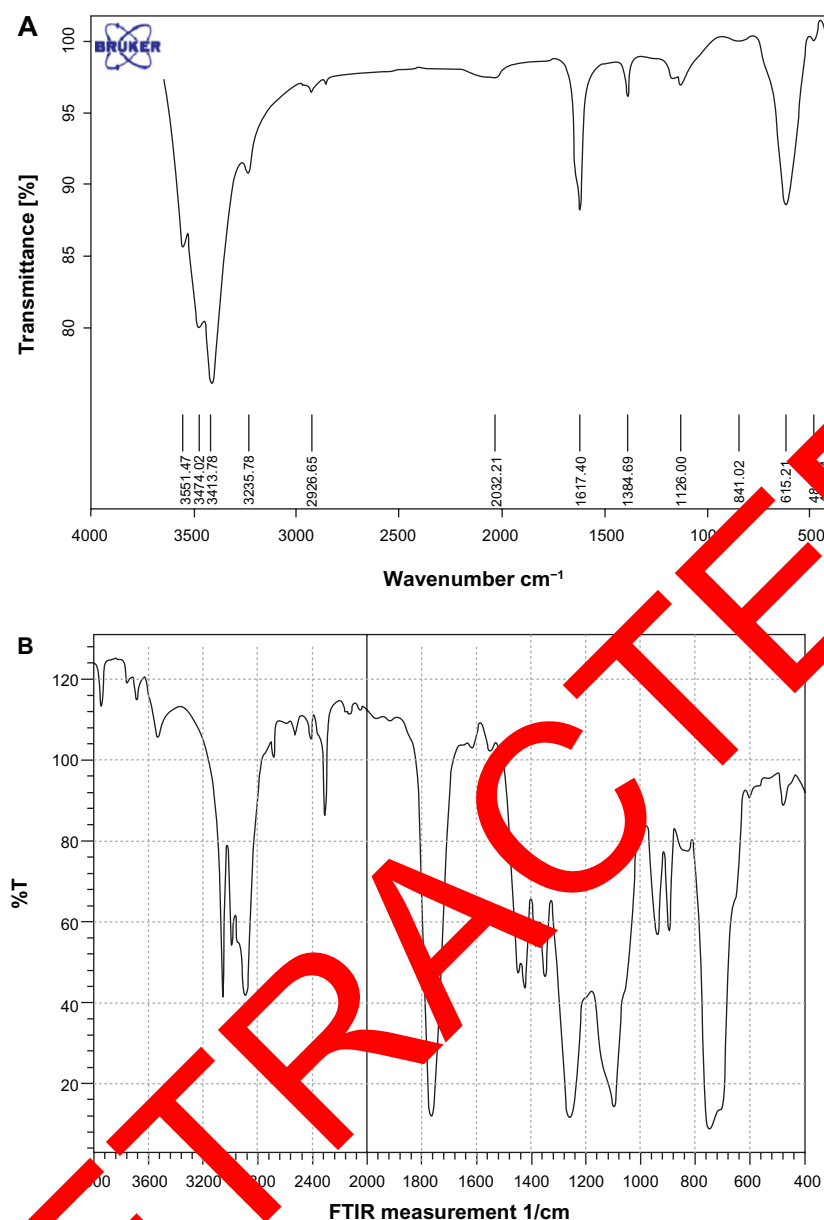


**Figure 12** Fourier transform infrared spectra of (A) pure  $\text{Fe}_3\text{O}_4$  nanoparticles and (B) PLGA-PEG copolymer nanoparticles.  
**Abbreviations:** PEG, poly (ethylene glycol); PLGA, poly (D, L-lactic-co-glycolic acid).

shows that absorption band at  $3509.9\text{ cm}^{-1}$  is assigned to terminal hydroxyl groups in the copolymer from which PEG homopolymer has been removed. The bands at  $3010\text{ cm}^{-1}$  and  $2955\text{ cm}^{-1}$  are due to C–H stretch of CH, and  $2885\text{ cm}^{-1}$  due to C–H stretch of CH. A strong band at  $1762.6\text{ cm}^{-1}$  is

assigned to C=O stretch. Absorption at  $1186\text{--}1089.6\text{ cm}^{-1}$  is due to C–O stretch.<sup>53</sup>

### $^1\text{H}$ NMR spectrum of PEG-PLGA copolymer

The basic chemical structure of PEG-PLGA copolymer is confirmed by  $^1\text{H}$  NMR spectra that were recorded in real-time with a Bruker DRX 300 spectrometer operating at 400 MHz. Chemical shift ( $\delta$ ) was measured in ppm using tetramethylsilane as an internal reference (Figure 13). One of the striking features is a large peak at 3.65 ppm, corresponding to the methylene groups of PEG. Overlapping doublets at 1.55 ppm are attributed to the methyl groups of the D-lactic

**Table I** Fourier transform infrared spectrum for  $\text{Fe}_3\text{O}_4$ <sup>84</sup>

System	Infrared bands ( $\text{cm}^{-1}$ )	Description
$\text{Fe}_3\text{O}_4$	440	Absorption band of Fe–O
	580	Absorption band of Fe–O
	620	Absorption band of Fe–O
	3402	–OH vibrations



**Figure 13** <sup>1</sup>H Nuclear magnetic resonance spectrum of PEG-PLGA copolymer.  
**Abbreviations:** PEG, poly (ethylene glycol); PLGA, poly (D, L-lactic-co-glycolic acid).

acid and L-lactic acid repeat units. The multiples at 5.1 and 4.8 ppm correspond to the lactic acid CH and the glycolic acid CH, respectively, with the high complexity of the two peaks resulting from different D-lactic, L-lactic, and glycolic acid sequences in the polymer backbone.

### Gel permeation chromatogram of PEG-PLGA copolymer

Molecular weights and molecular weight distribution of the obtained copolymer were determined by means of gel permeation chromatography (Figure 14).

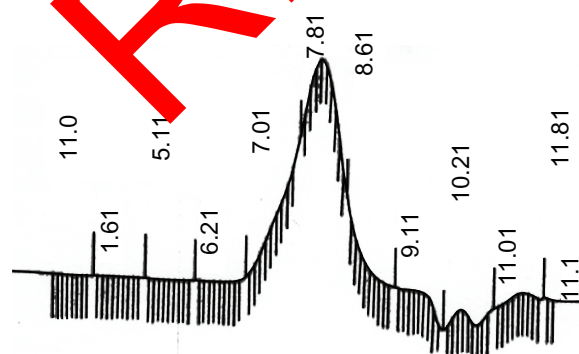


**Figure 14** Gel permeation chromatogram of the PEG-PLGA copolymer.  
**Abbreviations:** PEG, poly (ethylene glycol); PLGA, poly (D, L-lactic-co-glycolic acid).

The average molecular weight is 16,400. The unimodal mass distribution excluded the presence of PEG<sub>4000</sub> or PLGA<sup>55</sup> (molecular weight 16,400, number averaged molecular weight 7131, z-average molecular weight, 20,300, molecular weight at peak top 6850).

### Physicochemical characterization of nanoparticles

In order to investigate the physicochemical characterization of nanoparticles prepared by the double emulsion method (w/o/w), the nanoparticles were observed by SEM (Figure 9). From these micrographs, nanoparticles prepared with PLGA-PEG<sub>2000</sub>, PLGA-PEG<sub>3000</sub>, and PLGA-PEG<sub>4000</sub> containing doxorubicin were spherical in shape and uniform, with a size range of about 30–60 nm. The encapsulation efficiency values achieved for doxorubicin were influenced by the presence of PEG of different molecular weights in the PLGA chains (Table 2). Compared with PLGA-PEG<sub>4000</sub> nanoparticles (78%), PLGA-PEG<sub>3000</sub> and PLGA-PEG<sub>2000</sub> nanoparticles showed a lower encapsulation efficiency of 73% and 69.5%, respectively. The zeta potential values were obviously affected by the presence of different molecular weight PEG chains. Higher negative values were obtained for PLGA-PEG<sub>2000</sub> nanoparticles (−33.2 mV). A marked decrease

**Table 2** Physicochemical characterization and encapsulation efficiency of doxorubicin-loaded  $\text{Fe}_3\text{O}_4$  magnetic nanoparticles modified with PLGA-PEG<sub>2000</sub>, PLGA-PEG<sub>3000</sub>, and PLGA-PEG<sub>4000</sub>

$\text{Fe}_3\text{O}_4$ copolymer	Size (nm)	Zeta potential (mV)	Encapsulation efficiency (%)
$\text{Fe}_3\text{O}_4$ -PLGA-PEG <sub>2000</sub>	50 ± 15	-33.2 ± 0.9	69.5%
$\text{Fe}_3\text{O}_4$ -PLGA-PEG <sub>3000</sub>	35 ± 13	-22.5 ± 0.7	73%
$\text{Fe}_3\text{O}_4$ -PLGA-PEG <sub>4000</sub>	29 ± 11	-17.4 ± 0.5	78%

**Note:** Mean ± standard deviation (n = 3).

**Abbreviations:** PEG, poly (ethylene glycol); PLGA, poly (D, L-lactic-co-glycolic acid).

in the surface charge for PLGA-PEG<sub>4000</sub> nanoparticles (-17.4 mV) occurred.<sup>56</sup>

## In vitro release experiment

The in vitro doxorubicin release profiles were obtained by representing the percentage of doxorubicin release with respect to the amount of doxorubicin encapsulated. For three nanoparticles, doxorubicin release occurred in two phases: an initial burst release, with a significant amount of drug released within 12 hours, 30.1% for  $\text{Fe}_3\text{O}_4$  magnetic nanoparticles modified with PLGA-PEG<sub>4000</sub> nanoparticles, 25.6% for  $\text{Fe}_3\text{O}_4$  magnetic nanoparticles modified with PLGA-PEG<sub>3000</sub>, and 20.7% for  $\text{Fe}_3\text{O}_4$  magnetic nanoparticles modified with PLGA-PEG<sub>2000</sub> nanoparticles; and after 12 hours, the doxorubicin release profiles showed a sustained release pattern. The cumulative amount of doxorubicin release over 2 days was 83.4% from  $\text{Fe}_3\text{O}_4$ -PLGA-PEG<sub>4000</sub>, 70% from  $\text{Fe}_3\text{O}_4$ -PLGA-PEG<sub>3000</sub>, and 60.8% from  $\text{Fe}_3\text{O}_4$ -PLGA-PEG<sub>2000</sub> nanoparticles.<sup>57</sup> The doxorubicin release rate from the  $\text{Fe}_3\text{O}_4$ -PLGA-PEG nanoparticles was also pH-dependent and enhanced at pH 5.8. It is generally assumed that a drug is released by several processes, including diffusion through the polymer matrix, release by polymer degradation and solubilization and diffusion through microchannels that exist in the polymer matrix or are formed by erosion. The magnetic-coated copolymers prepared in the present work are AB triblock copolymers composed of hydrophilic A blocks (lactide-co-glycolide) and hydrophobic B blocks (central PEG). These copolymers are not soluble in water, but exhibit reverse thermal and pH-dependent gelation properties. Hydrolysis of the ester linkage in these polymers will cause the swelling to increase with time as hydrolysis proceeds. The gel becomes increasingly pH-sensitive as hydrolysis proceeds, and carboxylic acid groups are generated in the structure. Within about 6 days, we can consider that drug is released from the  $\text{Fe}_3\text{O}_4$ -PLGA-PEG nanoparticles by a diffusion mechanism in vitro. The swelling of the particles increases in acidic buffered solutions due to protonation of central

PEG groups and formation of positively charged chains in the polymer structure.

## In vitro cytotoxicity study

The MTT assay is an important method for evaluating the in vitro cytotoxicity of biomaterials. In the MTT assay, absorbance has a significant linear relationship with cell numbers. Corresponding optical images of cells are shown in Figure 15. The current work of the MTT assay showed that  $\text{Fe}_3\text{O}_4$ -PLGA-PEG<sub>4000</sub>-doxorubicin has dose-dependent and time-dependent cytotoxicity against the A549 lung cancer cell line ( $\text{IC}_{50}$  0.13–0.26 mg/mL). Also, the MTT assay showed that  $\text{Fe}_3\text{O}_4$ -PLGA-PEG<sub>3000</sub>-doxorubicin has dose-dependent and time-dependent cytotoxicity against the A549 lung cancer cell line ( $\text{IC}_{50}$  0.08 mg/mL), that  $\text{Fe}_3\text{O}_4$ -PLGA-PEG<sub>2000</sub>-doxorubicin has no dose-dependent cytotoxicity but does have time-dependent cytotoxicity against the A549 lung cancer cell line ( $\text{IC}_{50}$  0.17–0.48 mg/mL), and that pure doxorubicin has dose-dependent but not time-dependent cytotoxicity against this cell line ( $\text{IC}_{50}$  0.15–0.16 mg/mL). Therefore, there is a need for further study of doxorubicin-loaded  $\text{Fe}_3\text{O}_4$  magnetic nanoparticles modified with PLGA-PEG copolymers using the A549 lung cancer cell line in the future. However, the results of the current work demonstrate that the  $\text{IC}_{50}$  values for  $\text{Fe}_3\text{O}_4$ -PLGA-PEG<sub>4000</sub>-doxorubicin,  $\text{Fe}_3\text{O}_4$ -PLGA-PEG<sub>3000</sub>-doxorubicin,  $\text{Fe}_3\text{O}_4$ -PLGA-PEG<sub>2000</sub>-doxorubicin, and pure doxorubicin are about 0.18 mg/mL, 0.08 mg/mL, 0.13 mg/mL, and 0.15 mg/mL, respectively, in this cell line.

## Discussion

To reduce or minimize undesired interactions or undesired uptake into normal sites, a biodegradable nanocarrier has been developed for doxorubicin, wherein the amount and site of drug release is controlled by the structure of copolymer-coated magnetic nanoparticles and pH. This nanoparticle was designed and prepared so that the carrier can be used for targeting a broad range of solid tumors. For this purpose, AB triblock copolymers of PLGA-PEG were synthesized by



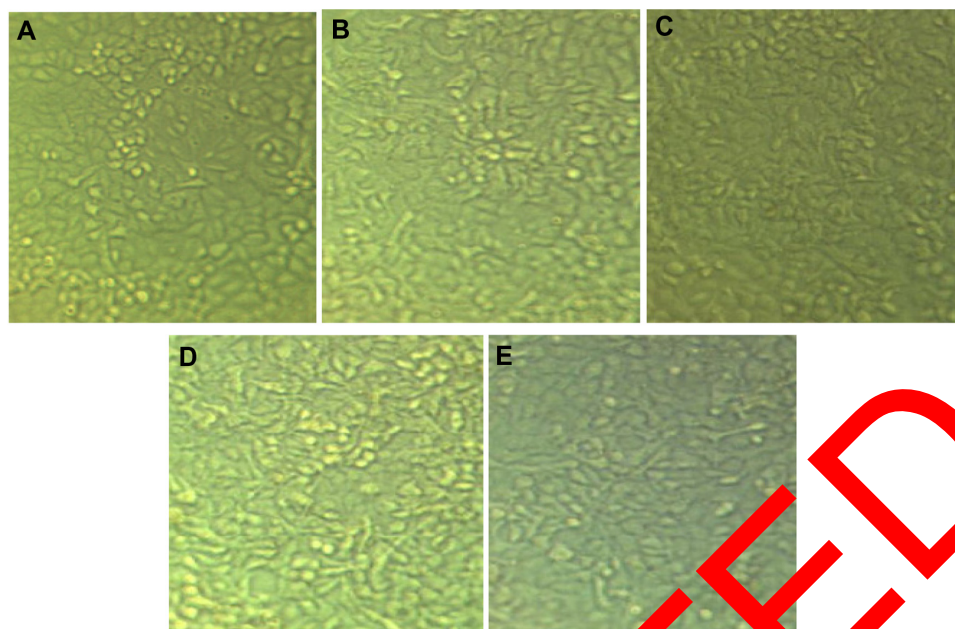


**Figure 15** Morphological effect of doxorubicin-loaded  $\text{Fe}_3\text{O}_4$  magnetic nanoparticles modified with PLGA-PEG copolymers on A549 lung cancer cell line after 24 hours of treatment. (A) Control cells, (B) doxorubicin-loaded  $\text{Fe}_3\text{O}_4$ -PLGA-PEG2000-Doxorubicin, (C)  $\text{Fe}_3\text{O}_4$ -PLGA-PEG<sub>3000</sub>-doxorubicin, (D)  $\text{Fe}_3\text{O}_4$ -PLGA-PEG<sub>4000</sub>-doxorubicin, and (E) pure doxorubicin.

**Abbreviations:** PEG, poly (ethylene glycol); PLGA, poly (D, L-lactic-co-glycolic acid).

ring opening polymerization of lactide and glycolide in the presence of PEG<sub>2000</sub>, PEG<sub>3000</sub>, and PEG<sub>4000</sub>.<sup>58–62</sup> The <sup>1</sup>H NMR and FTIR spectra were consistent with the structure of the PLGA-PEG copolymer. The molecular weight was determined by gel permeation chromatography. In this work, doxorubicin-loaded  $\text{Fe}_3\text{O}_4$  magnetic nanoparticles modified with PLGA-PEG copolymers were obtained. Encapsulation of doxorubicin in the nanoparticles was carried out by the double emulsion (w/o/w) technique.<sup>63–67</sup> For this purpose, the double emulsion (w/o/w) technique was considered the most appropriate method. However, the influence of other factors on entrapment efficiency using this technique is very complicated, and includes copolymer concentration in organic solution, volume of the inner aqueous phase, volume of the outer aqueous phase, doxorubicin concentration in the inner aqueous phase, the first homogenized speed and time, the second homogenized speed and time, and polyvinyl alcohol concentration.<sup>68,69</sup> The loading efficiency values achieved for doxorubicin were different between the various  $\text{Fe}_3\text{O}_4$ -PLGA-PEG nanoparticles, which could be attributable to the presence of different molecular weights of PEG in the PLGA chains, but the mechanism is indistinct. Compared with  $\text{Fe}_3\text{O}_4$ -PLGA-PEG<sub>4000</sub> nanoparticles,  $\text{Fe}_3\text{O}_4$ -PLGA-PEG<sub>3000</sub>, and  $\text{Fe}_3\text{O}_4$ -PLGA-PEG<sub>2000</sub> nanoparticles showed a marked decrease in encapsulation efficiency. The entrapment efficiency was 78%, 73%, and 69.5%, and the particle size was about 25–75 nm.

The results demonstrated in vitro that the doxorubicin-loaded  $\text{Fe}_3\text{O}_4$ -PLGA-PEG nanoparticles show pH sensitivity and can be applied for targeting extracellular pH, and could be an effective carrier for anticancer drugs. It is expected that at tumor pH, the doxorubicin-loaded nanoparticles made of  $\text{Fe}_3\text{O}_4$ -PLGA-PEG can show enhanced cytotoxicity compared with that at normal pH.<sup>70–74</sup>

In this paper, higher and faster doxorubicin release was observed for  $\text{Fe}_3\text{O}_4$ -PLGA-PEG<sub>4000</sub> nanoparticles than for  $\text{Fe}_3\text{O}_4$ -PLGA-PEG<sub>3000</sub> and  $\text{Fe}_3\text{O}_4$ -PLGA-PEG<sub>2000</sub> at 12 hours. This difference could be to the presence of PEG<sub>4000</sub> in the PLGA chains. In conclusion, modification of the magnetic nanoparticles could have potential benefit for drug delivery. Our results show that magnetic  $\text{Fe}_3\text{O}_4$ -PLGA-PEG nanoparticles could be an effective carrier for drug delivery.<sup>75–79</sup> The in vitro cytotoxicity test showed that the  $\text{Fe}_3\text{O}_4$ -PLGA:PEG<sub>4000</sub> magnetic nanoparticles had no cytotoxicity and were biocompatible, which means there is potential for biomedical application.<sup>80</sup> Also, the  $\text{IC}_{50}$  of doxorubicin-loaded  $\text{Fe}_3\text{O}_4$  magnetic nanoparticles modified with PLGA-PEG copolymers on an A549 lung cancer cell line was time-dependent.

## Conclusion

Superparamagnetic iron oxide nanoparticles were prepared using an improved chemical coprecipitation method and

then PLGA-PEG copolymer was used to encapsulate  $\text{Fe}_3\text{O}_4$  nanoparticles by an emulsion method (w/o/w). The results indicate that the copolymer chains effectively encapsulated the  $\text{Fe}_3\text{O}_4$  nanoparticles. Saturation magnetization was found to be 17.5 emu/g. These particles were employed in encapsulation of doxorubicin under mild conditions and could be used in drug delivery. An in vitro cytotoxicity study demonstrated that the PLGA-PEG nanoparticles and  $\text{Fe}_3\text{O}_4$ -PLGA-PEG nanoparticles had no cytotoxicity and were biocompatible. Our results suggest that supercritical fluid technology is a promising technique to produce drug-polymer magnetic composite nanoparticles for the design of controlled-release drug systems. Current work demonstrates that doxorubicin-loaded  $\text{Fe}_3\text{O}_4$  magnetic nanoparticles modified with PLGA-PEG triblock copolymers have potent time-dependent antigrowth effects in an A549 lung cancer cell line. Therefore, these nanoparticles could become a potent chemopreventive and chemotherapeutic system for lung cancer patients and constituents of this nanoparticles could be appropriate candidates for drug development. Future work will include an in vivo investigation of the targeting capability and effectiveness of these nanoparticles in the treatment of lung cancer.<sup>81,82</sup>

## Acknowledgments

The authors are grateful for the financial support of the Iran National Science Foundation, Drug Applied Research Center Tabriz University of Medical Sciences, and The Department of Medicinal Chemistry, Tabriz University of Medical Sciences.

## Disclosure

The authors report no conflicts of interest in this work.

## References

- Davaran S, Rashi V, Pouranvari B, Dadgarzadeh M, Haghshenas NM. Adriamycin release from poly (lactide-co-glycolide) polyethylene glycol nanoparticles: synthesis and in vitro characterization. *Int J Nanomedicine*. 2006;1:535–541.
- Gref R, Minamata Y, Peracchia MT, et al. Biodegradable long circulating polymeric nanoparticles. *Science*. 1994;263:1600–1630.
- Akbarzadeh A, Asgari D, Goganian AM, Khaksar Khiabani H, Davaran S. Synthesis of polymer-grafted VTES-modified  $\text{Fe}_3\text{O}_4$  nanoparticles for controlled drug release. [In press.]
- Li YP, Pei YY, Zhang XY, et al. PEGylated PLGA nanoparticles as protein carriers: synthesis, preparation and biodistribution in rats. *J Control Release*. 2001;71:203–211.
- Beletsi A, Panagi Z, Avgoustakis K. Biodistribution properties of nanoparticles based on mixtures of PLGA with PLGA-PEG diblock copolymers. *Int J Pharm*. 2005;298:233–241.
- Birnbaum DT, Brannon-Peppas L. Microparticle drug delivery systems. In: Brown DM, editor. *Drug Delivery Systems in Cancer Therapy*. Totowa, NJ: Humana Press; 2004.
- Eatock MM, Schätzlein A, Kaye SB. Tumor vasculature as a target for anticancer therapy. *Cancer Treat Rev*. 2000;26:191–204.
- Avgoustakis K, Beletsi A, Panagi Z, et al. Effect of copolymer composition on the physicochemical characteristics, in vitro stability, and biodistribution of PLGA-mPEG nanoparticles. *Int J Pharm*. 2003;259:115–127.
- Jeong Y, Nah JW, Lee HC, et al. Adriamycin release from flower-type polymeric micelles based on star-block copolymer composed of poly ( $\gamma$ -benzyl L-glutamate) as the hydrophobic part and poly(ethylene oxide) as the hydrophilic part. *Int J Pharm*. 1999;188:49–58.
- Kwon GS, Naito M, Yokoyama M, et al. Physical entrapment of adriamycin in AB block copolymer micelle. *Pharm Res*. 1995;12:192–195.
- Li YP, Pei YY, Zhang XY, et al. PEGylated PLGA nanoparticles as protein carriers: synthesis, preparation and biodistribution in rats. *J Control Release*. 2001;71:203–211.
- Mitra S, Gaur U, Ghosh PC, et al. Tumor targeted delivery of encapsulated dextran-doxorubicin conjugates using chitosan nanoparticles as carrier. *J Control Release*. 2001;74:311–323.
- Na K, Lee ES, Bae YH. Adriamycin loaded poly (vinyl acetate)/surfactant conjugate nanoparticles responding to tumor pH: pH-dependent cell interaction, internalization and cytotoxicity. *J Control Release*. 2003;87:3–13.
- Orive G, Hernández RM, Escalante AR, et al. Micro and nano drug delivery systems in cancer therapy. *Cancer Ther*. 2003;3:131–138.
- Panyam J, Labhasetwar V. Biodegradable nanoparticles for drug and gene delivery to cells and tissue. *Adv Drug Deliv Rev*. 2003;55:329–347.
- Peppas LB, Blanchard JO. Nanoparticle and targeted systems for cancer therapy. *Adv Drug Deliv Rev*. 2004;56:1649–1659.
- Reichmanis R, Moghimi S, Hodivala-Dilk K. Nanoparticle-mediated gene delivery to tumor vasculature. *Trends Mol Med*. 2003;9:2–4.
- Kataoka F, Tokunaga H, Ichikawa H, et al. In vitro cellular accumulation of gadolinium incorporated into chitosane nanoparticles designed for neutron-capture therapy of cancer. *Eur J Pharm Biopharm*. 2002;59:15–25.
- Sledge G, Miller K. exploiting the hallmarks of cancer: the future treatment of breast cancer. *Eur J Cancer*. 2003;39:1668–1675.
- Stubbs M, McSheely PMJ, Griffiths JR, et al. Causes and consequences of tumor acidity and implications for treatment. *Mol Med Today*. 2000;6:15–19.
- Tannock IF, Rotin D. Acid pH in tumors and its potential for therapeutic exploitation. *Cancer Res*. 1989;49:4373–4384.
- Teicher BA. Molecular targets and cancer therapeutics: discovery, development and clinical validation. *Drug Resist Updat*. 2000;3:67–73.
- Yoo HS, Lee KH, Oh JE, Park TG. In vitro and in vivo anti-tumor activities of nanoparticles based on doxorubicin-PLGA conjugates. *J Control Release*. 2000;68:419–431.
- Krizová J, Spanová A, Rittich B, Horák D. Magnetic hydrophilic methacrylate-based polymer microspheres for genomic DNA isolation. *J Chromatogr A*. 2005;1064:247–253.
- Beletsi A, Leontiadis L, Klepetsanis P, Ithakissios DS, Avgoustakis K. Effect of preparative variables on the properties of PLGA-mPEG copolymers related to their applications in controlled drug delivery. *Int J Pharm*. 1999;182:187–197.
- Yoo HS, Park TG. Biodegradable polymeric micelles composed of doxorubicin conjugated PLGA-PEG block copolymer. *J Control Release*. 2001;70:63–70.
- Kataoka K, Kwon G, Yokoyama M, Okano T, Sakurai Y. Block copolymer micelles as vehicles for drug delivery. *J Control Release*. 1992;24:119–132.
- Kwon GS, Okano T. Polymeric micelle as new drug carriers. *Adv Drug Del Rev*. 1996;16:107–116.
- Kwon G, Naito M, Yokoyama M, Okano T, Sakurai Y, Kataoka K. Block copolymer micelles for drug delivery: loading and release of doxorubicin. *J Control Release*. 1997;48:195–201.
- Kwon GS, Naito M, Yokoyama M, Okano T, Sakurai Y, Kataoka K. Physical entrapment of adriamycin in AB block copolymer micelles. *Pharm Res*. 1995;12:192–195.

31. Yokoyama M, Kwon GS, Okano T, Sakurai Y, Seto T, Kataoka K. Preparation of micelle-forming polymer-drug conjugates. *Bioconjug Chem.* 1992;3:295–301.
32. Duncan R. Drug-polymer conjugates: potential for improved chemotherapy. *Anticancer Drugs.* 1992;3:175–210.
33. Minko T, Kopecková P, Pozharov V, Kopecek J. HPMA copolymer bound adriamycin overcomes MDR1 gene encoded resistance in a human ovarian carcinoma cell line. *J Control Release.* 1998;54:223–233.
34. Colin de Verdière A, Dubernet C, Nemati F, Poupon MF, Puisieux F, Couvreur P. Uptake of doxorubicin from loaded nanoparticles in multidrug resistant leukemic murine cells. *Cancer Chemother Pharmacol.* 1994;33:504–508.
35. Malmsten M, Lindman B. Self-assembly in aqueous block copolymer solution. *Macromolecules.* 1992;25:5440–5445.
36. Jeong JH, Lim DW, Han DK, Park TG. Synthesis, characterization and protein adsorption behaviors of PLGA/PEG di-block co-polymer blend films. *Colloids Surf B Biointerfaces.* 2000;18:371–379.
37. Yuan M, Wang Y, Li X, Xiong C, Deng X. Polymerization of lactides and lactones. 10. Synthesis, characterization, and application of amino-terminated poly (ethylene glycol)-co-poly ([ε]-caprolactone) block copolymer. *Macromolecules.* 2000;33:1613–1617.
38. Yoo HS, Oh JE, Lee KH, Park TG. Biodegradable nanoparticles containing doxorubicin-PLGA conjugates for sustained release. *Pharm Res.* 1999;16:1114–1118.
39. Zhao C, Winnik M, Reiss G, Croucher M. Fluorescence probe technique used to study micelle formation in water-soluble block copolymers. *Langmuir.* 1990;6:514–516.
40. Kedar E, Algi O, Golod G, Babai I, Barenholz Y. Delivery of cytokines by liposomes. III. Liposome-encapsulated GM-CSF and TNF-α show improved pharmacokinetics and biological activity and reduced toxicity in mice. *J Immunother.* 1997;20:180–193.
41. Yasui K, Nakamura Y. Positively charged liposomes containing tumor necrosis factor in solid tumors. *Biol Pharm Bull.* 2003;50:321–322.
42. Zambaux MF, Bonneaux F, Gref R, Dellacherie E, Vigneron C. Preparation and characterization of protein C loaded PLGA nanoparticles. *J Control Release.* 1999;60:179–188.
43. Stolnik S, Illum L, Davis SS. Long circulating microparticle drug carriers. *Adv Drug Del Rev.* 1995;16:195–207.
44. Yang J, Park SB, Yoon H-G, Hun YM, Chaam P. Preparation of poly ε-caprolactone nanoparticles containing magnetite for magnetic drug carrier. *Int J Pharm.* 2006;324:189–190.
45. Savva M, Duda E, Huang L. A genetically modified recombinant tumor necrosis factor-α conjugated to the distal terminals of liposomal surface grafted poly-ethylene glycol chains. *Int J Pharm.* 1999;184:45–51.
46. Yuyama Y, Tsujimoto M, Fujimoto Y, Oku N. Potential usage of thermosensitive liposomes for site-specific delivery of cytokines. *Cancer Lett.* 2000;157:77.
47. Carmichael J, Duffraff W, Gaudar AF, Minna JD, Mitchell JB. Evaluation of a tetrazolium-based semiautomated colorimetric assay: assessment of inter-assay variability testing. *Cancer Res.* 1987;47(4):936–942.
48. Mohammad Nosratollah Z, Mohammad R, Abbas A, Java R. The inhibitory effect of Curcuma longa extract on telomerase activity in A549 lung cancer cell line. *African Journal of Biotechnology.* 2010;9:912–919.
49. Allemann E, Gurny R, Doelker E. Drug-loaded nanoparticles – preparation methods and drug targeting issues. *Eur J Pharm Biopharm.* 1993;39:173–191.
50. Gref R, Minamitake Y, Peracchia MT, Trubetskoy V, Torchilin V, Langer R. Biodegradable long-circulating polymeric nanospheres. *Science.* 1994;263:1600–1603.
51. Tobio M, Gref R, Sanchez A, Langer R, Alonso MJ. Stealth PLA-PEG nanoparticles as protein carriers for nasal administration. *Pharm Res.* 1998;15:270–275.
52. Quellec P, Gref R, Perrin L, et al. Protein encapsulation within polyethylene glycol-coated nanospheres. I. Physicochemical characterization. *J Biomed Mater Res.* 1998;42:45–54.
53. Peracchia MT, Vauthier C, Passirani C, Couvreur P, Labarre D. Complement consumption by poly(ethylene glycol) in different conformations chemically coupled to poly-(isobutyl 2-cyanoacrylate) nanoparticles. *Life Sci.* 1997;61:749–761.
54. Stolnik S, Dunn SE, Garnett MC, et al. Surface modification of poly(lactide-co-glycolide) nanoparticles by biodegradable poly(lactide)-poly(ethylene glycol) copolymer. *Pharm Res.* 1994;11:1800–1808.
55. Bazile D, Prud'homme C, Bassoullet MT, Marlard M, Spenlehauer G, Veillard M. Stealth Me. PEG-PLA nanoparticles avoid uptake by the mononuclear phagocyte system. *J Pharm Sci.* 1995;84:493–498.
56. Peracchia MT, Gref R, Minamitake Y, Domb A, Lotan N, Langer R. PEG-coated nanoparticles from amphiphilic diblock and multiblock copolymer: investigation of their encapsulation and release characteristics. *J Control Release.* 1997;46:223–232.
57. Jeong B, Bae YH, Kim SW. Drug release from biodegradable injectable thermosensitive hydrogel of PEG-PLGA-PEG triblock copolymer. *J Control Release.* 2000;63:155–163.
58. Lamprecht A, Ubrich N, Hogueiro Pérez M, Lehr C, Hoffman M, Maincent P. Biodegradable monodispersed nanoparticles prepared by pressure homogenization/emulsification. *Int J Pharm.* 1999;184:97–105.
59. Iwata M, McCarty JW. Preparation of multi-phase microspheres of poly (lactic acid) and poly (lactic-co-glycolic acid) containing a w/o emulsion by a multiphase solvent evaporation technique. *J Microencapsul.* 1992;9:201–214.
60. Blanco MD, Alonso MJ. Development and characterization of protein-loaded poly (lactide-co-glycolide) nanospheres. *Eur J Pharm Biopharm.* 1999;43:287–294.
61. Langer R, Preat V. Polymeric nanoparticles as delivery system for influenza virus glycoproteins. *J Control Release.* 1998;54:15–27.
62. Peterson PL. A simplification of the protein assay method of Lowry et al which is more generally applicable. *Anal Biochem.* 1977;83:546–556.
63. Hrkach JS, Peracchia MT, Domb A, Lotan N, Langer R. Nanotechnology for biomaterials engineering: structural characterization of amphiphilic polymeric nanoparticles by 1H-NMR spectroscopy. *Biomaterials.* 1997;18:27–30.
64. Sah H. Protein behavior at the water/methylene chloride interface. *J Pharm Sci.* 1999;88:1320–1325.
65. Sah H. Stabilization of protein against methylene chloride water interface-induced denaturation and aggregation. *J Control Release.* 1999;58:143–151.
66. Velge-Roussel F, Breton P, Guillon X, Lescure F, Bout D, Hoebeke J. Immunochemical characterization of antibody-coated nanoparticles. *Experientia.* 1996;52:803–806.
67. Armstrong TI, Davies MC, Illum L. Human serum albumin as a probe for protein adsorption to nanoparticles. *J Drug Target.* 1997;4:389–398.
68. Park TG. Degradation of poly (DL-lactic) microsphere: effect of molecular weight. *J Control Release.* 1994;30:161–173.
69. Yoo HS, Park TG. In vitro and in vivo anti-tumor activities of nanoparticles based on doxorubicin-PLGA conjugates. *J Control Release.* 2000;68:419–431.
70. Mahkam M, Assadi MG, Ramesh M, Davaran S. Linear type azo containing polyurethanes for colon-specific drug delivery. *J Bioact Compat Polym.* 2004;19:45–53.
71. Garjani MR, Davaran S, Rashidi MR, Malek N. Protective effects of some azo derivatives of 5-amino salicylic acid and their PEGylated prodrugs an acetic acid induced rat colitis. *Daru.* 2004;12:24–30.
72. Davaran S, Rashidi MR, Hashemi M. Synthesis and hydrolytic behaviour of 2-mercaptoethyl ibuprofenate-polyethylene glycol conjugate as a novel transdermal prodrug. *J Pharm Pharmacol.* 2003;55:513–517.

73. Davaran S, Rashidi MR, Hashemi M. Synthesis and characterization of methacrylic derivatives of 5-amino salicylic acid with pH-sensitive swelling properties. *AAPS PharmSciTech*. 2001;2:29.
74. Davaran S, Rashidi MR, Ershadpour B. Preparation of acrylic-type hydrogels containing 5-amino salicylic acid. *J Pharm Sci*. 2001;4: 55–63.
75. Davaran S, Hanaee J, Khosrawi A. Release of 5-amino salicylic acid from acrylic type polymeric prodrugs designed for colon-specific drug delivery. *J Control Release*. 1998;58:279–287.
76. Davaran S, Entezami AA. Hydrophilic copolymers prepared from acrylic type derivatives of ibuprofen containing hydrolyzable thioester bond. *Eur Polym J*. 1998;34:187–192.
77. Davaran S, Entezami AA. Synthesis and hydrolysis of polyurethanes containing ibuprofen groups. *J Bioact Compat Polym*. 1997;12: 47–58.
78. Davaran S, Entezami AA. Acrylic type polymers containing ibuprofen and indomethacin with difunctional spacer group: synthesis and hydrolysis. *J Control Release*. 1997;47:41–79.
79. Nasir Tabrizi MH, Davaran S, Entezami AA. Synthesis of diclofenac polymeric prodrugs and their hydrolysis reactivity. *Iran Polym J*. 1996;5: 243–249.
80. Mahmoudi M, Sant S, Wang B, Laurent S, Sen T. Superparamagnetic iron oxide nanoparticles (SPIONs): Development, surface modification and applications in chemotherapy. *Adv Drug Deliv Rev*. 2011;63: 24–46.
81. Davaran S, Entezami AA. Synthesis and hydrolysis of modified poly vinyl alcohols containing ibuprofen pendent groups. *Iran Polym J*. 1996;5:188–191.
82. Davaran S, Entezami AA. A review on application of polymers in new drug delivery systems. *Iran Polym J*. 1994;6:273–289.

RETRACTED

### International Journal of Nanomedicine

### Publish your work in this journal

The International Journal of Nanomedicine is an international, peer-reviewed journal focusing on the application of nanotechnology in diagnostics, therapeutics, and drug delivery systems throughout the biomedical field. This journal is indexed on PubMed Central, MedLine, CAS, SciSearch®, Current Contents®/Clinical Medicine,

Submit your manuscript here: <http://www.dovepress.com/international-journal-of-nanomedicine-journal>

Dovepress

Journal Citation Reports/Science Edition, EMBase, Scopus and the Elsevier Bibliographic databases. The manuscript management system is completely online and includes a very quick and fair peer-review system, which is all easy to use. Visit <http://www.dovepress.com/testimonials.php> to read real quotes from published authors.